Theory of correlation in a network with synaptic depression

Yasuhiko Igarashi,[1] Masafumi Oizumi,[2,3] and Masato Okada[1,3,*]

[1]*Graduate School of Frontier Sciences, The University of Tokyo, Chiba 277-5861, Japan*
[2]*Research Fellow of the Japan Society for the Promotion of Science, 2-1 Hirosawa, Wako 351-0198, Japan*
[3]*RIKEN Brain Science Institute 2-1 Hirosawa, Wako 351-0198, Japan*

Synaptic depression affects not only the mean responses of neurons but also the correlation of response variability in neural populations. Although previous studies have constructed a theory of correlation in a spiking neuron model by using the mean-field theory framework, synaptic depression has not been taken into consideration. We expanded the previous theoretical framework in this study to spiking neuron models with short-term synaptic depression. On the basis of this theory we analytically calculated neural correlations in a ring attractor network with Mexican-hat-type connectivity, which was used as a model of the primary visual cortex. The results revealed that synaptic depression reduces neural correlation, which could be beneficial for sensory coding. Furthermore, our study opens the way for theoretical studies on the effect of interaction change on the linear response function in large stochastic networks.

PACS number(s): 84.35.+i, 02.50.−r

I. INTRODUCTION

A marked feature of synaptic transmission between neocortical neurons is the pronounced frequency dependence of synaptic responses on presynaptic spike trains [1]. High-frequency input reduces the efficacy of signal transmission due to the depletion of neurotransmitters. Short-term synaptic depression, which has been described in detail by using a phenomenological model [2,3], occurs over milliseconds to minutes in various regions such as the primary visual cortex and the hippocampus [4–6]. Because of its rapid effects, short-term synaptic depression enables synapses to perform critical computational functions in neural circuits such as belief adaptation to external stimuli and short-term memory [7–9].

To evaluate how synaptic depression affects the amount of information on stimuli that can be extracted from noisy neural activities, we need to investigate the effects of synaptic depression not only on the firing rates but also on neural correlations. Even small correlations between neurons can greatly change the amount of information conveyed by the activities of the neural population and consequently affect the accuracy of sensory discriminations [10–17]. Similar to the derivation of the linear-response function for an Ising system with transition rates [18,19], some researchers have gone beyond mean-field theory and developed such a theory of correlation in a spiking neuron model including a time course for postsynaptic potential and refractory properties [20–23]. However, short-term synaptic depression, which rapidly changes the interaction between neurons, has not been taken into account and the effect of the interaction change on neural correlation remains unknown. Here we expanded the previous theoretical framework to spiking neuron models with short-term synaptic depression.

We investigated the effects of synaptic depression on the macroscopic behavior of stochastic neural networks in previous studies, viz., the firing rates [24,25]. Dynamical mean-field equations were derived for these networks by taking

the average of two stochastic variables: a firing-state variable and a synaptic variable. Because synaptic depression is activity dependent and leads to the independence of the two stochastic variables, the average product of these variables is decoupled as the product of their averages and we can then calculate the firing rates. We used the independence in this study to calculate the neural correlations and constructed a theoretical framework for analytically calculating correlations of neural activities in a neural network with synaptic depression.

We studied how short-term synaptic depression affects neural correlations for a ring attractor network with Mexican-hat-type connectivity using this theory as an example, which is known as a neural network model of the primary visual cortex [13,17,26,27]. We analytically calculated the neural correlations and investigated not only the effects of synaptic depression at the single cell level [28] but also what influence changes in single neurons have on network activity as a whole. We found that synaptic depression substantially reduces neural correlations. We also demonstrated that this reduction in neural correlations due to synaptic depression can improve the accuracy of population coding, even though the signal strength, viz., the mean firing rates, is reduced by synaptic depression.

II. MODEL

We used a discrete time version of a spike response model with threshold noise [23,29]. The network consists of N neurons, which take either a resting state $S = 0$ or a firing state $S = 1$. The state of every neuron S_i is stochastically updated in parallel. The probability that S_i takes the 0 or 1 state depends on the membrane potential u_i:

$$P[S_i(t) = 1] \equiv g[u_i(t)],$$
$$P[S_i(t) = 0] = 1 - P[S_i(t) = 1], \tag{1}$$

where g is the "escape function" [30], which monotonically increases and is a differentiable function that takes values

*okada@k.u-tokyo.ac.jp

between 0 and 1. The membrane potential u_i is determined by the past spike histories of N neurons as

$$u_i(t) = \sum_{\tau=1}^{\infty} \sum_{j \neq i} J_{ij}\epsilon_{ij}(\tau)[2x_j(t-\tau)S_j(t-\tau) - 1] + h_i + u_r,$$

$$(2)$$

where $\epsilon_{ij}(\tau)$ describes the time course of a postsynaptic potential evoked by the firing of presynaptic neurons, h_i is an input potential, and u_r is a resting potential. We have not taken into account the effect of refractoriness to simplify the network model and investigate the effect of synaptic plasticity on the correlation between neural activities. The synaptic connection $J_{ij}(t)$ $[=J_{ij}x_j(t)]$ in this model dynamically changes with the efficacy of signal transmission at the jth neuron $x_j(t)$. $x_j(t)$ dynamically changes with synaptic depression and is determined by both itself and the corresponding neuron state at the preceding time $t-1$:

$$x_i(t+1) = x_i(t) + \frac{1 - x_i(t)}{\tau_D} - Ux_i(t)S_i(t). \quad (3)$$

The phenomenological model of synaptic depression described by Eq. (3) has previously been proposed by several researchers [2,3]. The jth neuron, which is called a presynaptic neuron, exhausts neurotransmitters when it transmits signals. The efficacy of signal transmission at presynaptic neuron j at time t decreases by a certain fraction $Ux_j(t-1)$ $(0 < U \leqslant 1)$ after the presynaptic neuron $S_j(t-1) = 1$ is fired and it recovers with time constant τ_D $(\tau_D \geqslant 1)$, as shown in Eq. (3).

III. THEORY OF CORRELATIONS

A. Instantaneous firing rate and synaptic efficacy

First we consider the noise average of neuronal states and synaptic variables, which are denoted by $\langle S_i(t) \rangle$ for the former and $\langle x_i(t) \rangle$ for the latter. We call these values the instantaneous firing rate and synaptic efficacy at time t. We derive dynamical mean-field equations in this section for a network with synaptic depression by taking the average of two stochastic variables: a firing-state variable $S(t)$ and a synaptic variable $x(t)$. The average product of the variables in these equations is decoupled as the product of their averages because the stochastic variables are independent in the limit of $N \to \infty$ [25]. We derived the instantaneous firing rate and synaptic efficacy at a steady state by using these equations.

The noise average of a function $\langle f \rangle$ is defined as

$$\langle f(\mathbf{S}^t, \mathbf{S}^{t-1}, \ldots, \mathbf{S}^0) \rangle \equiv \sum_{\mathbf{S}^t} \sum_{\mathbf{S}^{t-1}} \cdots \sum_{\mathbf{S}^0} f(\mathbf{S}^t, \mathbf{S}^{t-1}, \ldots, \mathbf{S}^0)$$

$$\times P(\mathbf{S}^t, \mathbf{S}^{t-1}, \ldots, \mathbf{S}^0), \quad (4)$$

where $\mathbf{S}^t$ represents the spike pattern of N neurons at time t and $\sum_{\mathbf{S}^t}$ represents the summation over all possible configurations $\mathbf{S}^t$. $P(\mathbf{S}^t, \mathbf{S}^{t-1}, \ldots, \mathbf{S}^0)$ is the probability of finding a system in a state $\{\mathbf{S}^t, \mathbf{S}^{t-1}, \ldots, \mathbf{S}^0\}$. $P(\mathbf{S}^t, \mathbf{S}^{t-1}, \ldots, \mathbf{S}^0)$ is described by the following master equation:

$$P(\mathbf{S}^t, \mathbf{S}^{t-1}, \ldots, \mathbf{S}^0) = W(\mathbf{S}^t | \mathbf{S}^{t-1}, \mathbf{S}^{t-2}, \ldots, \mathbf{S}^0)$$

$$\times P(\mathbf{S}^{t-1}, \mathbf{S}^{t-2}, \ldots, \mathbf{S}^0), \quad (5)$$

where $W(\mathbf{S}^t | \mathbf{S}^{t-1}, \mathbf{S}^{t-2}, \ldots, \mathbf{S}^0)$ is the transition probability, which is determined by the update rule Eq. (1)

$$W(\mathbf{S}^t | \mathbf{S}^{t-1}, \mathbf{S}^{t-2}, \ldots, \mathbf{S}^0)$$

$$= \prod_{i=1}^{N} \frac{1 + [2S_i(t) - 1]\{2g[u_i(t)] - 1\}}{2}. \quad (6)$$

To simplify the equation, $\{\mathbf{S}^{t-1}, \mathbf{S}^{t-2}, \ldots, \mathbf{S}^0\}$ are denoted by Y^{t-1}.

By using Eq. (5), the instantaneous firing rate at time t $[\langle S_i(t) \rangle]$ can be computed as

$$\langle S_i(t) \rangle = \sum_{Y^{t-1}} P(Y^{t-1}) \sum_{\mathbf{S}^t} S_i(t) W(\mathbf{S}^t | Y^{t-1}) = \langle g[u_i(t)] \rangle, \quad (7)$$

where $\sum_{Y^{t-1}}$ represents the summation over all possible configurations of the past spike histories Y^{t-1}.

We derived microscopic dynamical mean-field equations by first taking the noise average of the firing-state variable at time t [Eq. (7)]. Taylor expansion provides us with

$$\langle S_i(t) \rangle = \Big\langle g[\langle u_i(t) \rangle] + g'[\langle u_i(t) \rangle]\delta u_i(t)$$

$$+ \tfrac{1}{2}g''[\langle u_i(t) \rangle][\delta u_i(t)]^2 + \cdots \Big\rangle$$

$$= g[\langle u_i(t) \rangle] + \Big\langle \tfrac{1}{2}g''[\langle u_i(t) \rangle][\delta u_i(t)]^2 \Big\rangle + \cdots, \quad (8)$$

where we define $\delta u_i(t) = u_i(t) - \langle u_i(t) \rangle$, $g'(u) = dg(u)/dt$, and $g''(u) = d^2g(u)/dt^2$. When each neuron is connected to a number of neurons of order N and connections J_{ij} are all of order $1/N$, $\langle [\delta u_i(t)]^2 \rangle$ are of order $1/N$ (see Appendix A). The second order and the higher-order terms of Eq. (8) in such a situation are no more than order $1/N$. Hence, considering the limit of $N \to \infty$, one obtains leading order

$$\langle S_i(t) \rangle = g\left\{ \sum_{\tau=1}^{\infty} \sum_{j \neq i} J_{ij}\epsilon_{ij}(\tau)[2\langle x_j(t-\tau)S_j(t-\tau) \rangle - 1] \right.$$

$$\left. + h_i + u_r \right\}. \quad (9)$$

We take advantage of the independence of $x_j(t)$ and $S_j(t)$ in the limit of large networks $N \to \infty$ [25], and thereby obtain the dynamical mean-field equations for $\langle S_i(t) \rangle$:

$$\langle S_i(t) \rangle = g\left\{ \sum_{\tau=1}^{\infty} \sum_{j \neq i} J_{ij}\epsilon_{ij}(\tau)[2\langle x_j(t-\tau) \rangle \langle S_j(t-\tau) \rangle - 1] \right.$$

$$\left. + h_i + u_r \right\}. \quad (10)$$

Similarly, we consider the noise average of Eq. (3) for the synaptic variable:

$$\langle x_i(t+1) \rangle = \langle x_i(t) \rangle + \frac{1 - \langle x_i(t) \rangle}{\tau_D} - U \langle x_i(t) \rangle \langle S_i(t) \rangle. \quad (11)$$

Equations (10) and (11) for the stochastic neural network model coincide with equations for an analog neural network

with synaptic depression [3,31,32]. We then obtain the microscopic steady-state equation for $\langle S_i \rangle$ and $\langle x_i \rangle$:

$$\langle S_i \rangle = g \left\{ \sum_{\tau=1}^{\infty} \sum_{j \neq i} J_{ij} \epsilon_{ij}(\tau)(2\langle x_j \rangle \langle S_j \rangle - 1) + h_i + u_r \right\}, \quad (12)$$

$$\langle x_i \rangle = \langle x_i \rangle + \frac{1 - \langle x_i \rangle}{\tau_D} - U \langle x_i \rangle \langle S_i \rangle, \quad (13)$$

where $\langle S_i \rangle = \lim_{t \to \infty} \langle S_i(t) \rangle$ and $\langle x_i \rangle = \lim_{t \to \infty} \langle x_i(t) \rangle$. The steady-state equation for noise average $\langle x_i \rangle$ is

$$\langle x_i \rangle = \frac{1}{1 + \gamma \langle S_i \rangle}, \quad \gamma = \tau_D U. \quad (14)$$

Finally, we obtain the microscopic steady-state equation for $\langle S_i \rangle$ in a network with synaptic depression

$$\langle S_i \rangle = g \left[\sum_{\tau=1}^{\infty} \sum_{j \neq i} J_{ij} \epsilon_{ij}(\tau) \left(2 \frac{\langle S_j \rangle}{1 + \gamma \langle S_j \rangle} - 1 \right) + h_i + u_r \right]. \quad (15)$$

According to Eq. (15), the steady state depends on γ ($= \tau_D U$), which ranges from 0 to U because of $0 < U \leqslant 1$ and $\tau_D \geqslant 1$ [3,25]. Therefore, we can easily figure out the effect of synaptic depression by varying γ. If we solve the self-consistent equation (15), we can obtain instantaneous firing rates $\langle S_i \rangle$ and synaptic efficacies at equilibrium $\langle x_i \rangle$.

B. Equal-time correlation functions

We derive autocorrelation functions and cross-correlation functions in this section and the one that follows it to calculate correlations between neural activities at equilibrium. As a synaptic variable x dynamically changes in this network model, we need to discuss not only correlations between the activities of cortical neurons but also those between neural activities and synaptic variables. We then have to derive and solve 15 types of equations to calculate neural correlations at equilibrium. We define neural correlation in this section and the next and briefly explain how the equations are derived. We present the technical details on the calculations in Appendix B.

Autocorrelation functions are defined as

$$\begin{aligned}
A_i^s(t, t+\tau) &\equiv \langle \delta S_i(t) \delta S_i(t+\tau) \rangle, \\
A_i^{sx}(t, t+\tau) &\equiv \langle \delta S_i(t) \delta x_i(t+\tau) \rangle, \\
A_i^{xs}(t, t+\tau) &\equiv \langle \delta x_i(t) \delta S_i(t+\tau) \rangle, \\
A_i^x(t, t+\tau) &\equiv \langle \delta x_i(t) \delta x_i(t+\tau) \rangle.
\end{aligned} \quad (16)$$

We also define cross-correlation functions as

$$\begin{aligned}
C_{ij}^s(t, t+\tau) &\equiv \langle \delta S_i(t) \delta S_j(t+\tau) \rangle, \\
C_{ij}^{sx}(t, t+\tau) &\equiv \langle \delta S_i(t) \delta x_j(t+\tau) \rangle, \\
C_{ij}^{xs}(t, t+\tau) &\equiv \langle \delta x_i(t) \delta S_j(t+\tau) \rangle, \\
C_{ij}^x(t, t+\tau) &\equiv \langle \delta x_i(t) \delta x_j(t+\tau) \rangle,
\end{aligned} \quad (17)$$

where $i \neq j$. We denote the autocorrelation functions and cross-correlation functions at equilibrium as

$$\begin{aligned}
A_i^s(\tau) &\equiv \lim_{t \to \infty} \langle \delta S_i(t) \delta S_i(t+\tau) \rangle, \\
A_i^{sx}(\tau) &\equiv \lim_{t \to \infty} \langle \delta S_i(t) \delta x_i(t+\tau) \rangle, \\
A_i^{xs}(\tau) &\equiv \lim_{t \to \infty} \langle \delta x_i(t) \delta S_i(t+\tau) \rangle, \\
A_i^x(\tau) &\equiv \lim_{t \to \infty} \langle \delta x_i(t) \delta x_i(t+\tau) \rangle,
\end{aligned} \quad (18)$$

$$\begin{aligned}
C_{ij}^s(\tau) &\equiv \lim_{t \to \infty} \langle \delta S_i(t) \delta S_j(t+\tau) \rangle, \\
C_{ij}^{sx}(\tau) &\equiv \lim_{t \to \infty} \langle \delta S_i(t) \delta x_j(t+\tau) \rangle, \\
C_{ij}^{xs}(\tau) &\equiv \lim_{t \to \infty} \langle \delta x_i(t) \delta S_j(t+\tau) \rangle, \\
C_{ij}^x(\tau) &\equiv \lim_{t \to \infty} \langle \delta x_i(t) \delta x_j(t+\tau) \rangle.
\end{aligned} \quad (19)$$

We use instantaneous firing rate $\langle S_i \rangle$ and synaptic efficacy $\langle x_i \rangle$ in a steady state to calculate the equilibrium values of autocorrelation functions and cross-correlation functions in this and the following section.

We derive the equal-time autocorrelation functions $A_i^s(0)$, $A_i^{sx}(0)$, $A_i^{xs}(0)$, $A_i^x(0)$, and the equal-time cross-correlation functions $C_{ij}^s(0)$, $C_{ij}^{sx}(0)$, $C_{ij}^{xs}(0)$, $C_{ij}^x(0)$ in this section.

First, we calculate $A_i^s(0)$ at equilibrium. Since the neural network consists of binary neurons, $S_i = 0, 1$, we can derive $S_i^2 = S_i$. Using this equation yields

$$A_i^s(0) = \langle S_i \rangle (1 - \langle S_i \rangle). \quad (20)$$

The equal-time cross-correlation functions between $S_i(t)$ and $S_j(t)$ ($j \neq i$), that is, $C_{ij}^s(0)$, can be written as

$$\begin{aligned}
C_{ij}^s(t,t) &= \langle S_i(t) S_j(t) \rangle - \langle S_i(t) \rangle \langle S_j(t) \rangle \\
&= \sum_{Y^{t-1}} \left[\mathbf{P}(Y^{t-1}) \sum_{\mathbf{S}^t} S_i(t) S_j(t) \mathbf{W}(\mathbf{S}^t | Y^{t-1}) \right. \\
&\quad \left. - \langle S_i(t) \rangle \langle S_j(t) \rangle \right] \\
&= \langle g[u_i(t)] g[u_j(t)] \rangle - \langle g[u_i(t)] \rangle \langle g[u_j(t)] \rangle. \quad (21)
\end{aligned}$$

By expanding $g[u_i(t)]$ around the noise average of $\hat{u}_i$ and taking limit $t \to \infty$, we obtain (see Appendix B for details)

$$\begin{aligned}
C_{ij}^s(0) &= \sum_{\tau,\tau'} \sum_{k \neq i} \sum_{l \neq j,k} \tilde{J}_{ik}(\tau) \tilde{J}_{jl}(\tau') Z_{kl}(\tau - \tau') \\
&\quad + \sum_{\tau,\tau'}^{\infty} \sum_{k \neq i} \tilde{J}_{ik}(\tau) \tilde{J}_{jk}(\tau') Z_k(\tau - \tau'), \quad (22)
\end{aligned}$$

where we denote $\tilde{J}_{ik}(\tau) = 2g'(\langle u_i \rangle) J_{ik} \epsilon_{ik}(\tau)$ and

$$\begin{aligned}
Z_{kl}(t, t+\tau) &\equiv \langle \delta[x_k(t) S_k(t)] \delta[x_l(t+\tau) S_l(t+\tau)] \rangle, \\
Z_{kl}(\tau) &\equiv \lim_{t \to \infty} Z_{kl}(t, t+\tau), \quad (23)
\end{aligned}$$

$$\begin{aligned}
Z_k(t, t+\tau) &\equiv \langle \delta[x_k(t) S_k(t)] \delta[x_k(t+\tau) S_k(t+\tau)] \rangle. \\
Z_k(\tau) &\equiv \lim_{t \to \infty} Z_k(t, t+\tau). \quad (24)
\end{aligned}$$

We evaluate $Z_{kl}(\tau)$ and $Z_k(\tau)$ at equilibrium and derive (see Appendix B for details)

$$Z_{kl}(\tau) = C_{kl}^s(\tau)\langle x_k\rangle\langle x_l\rangle + C_{kl}^{sx}(\tau)\langle x_k\rangle\langle S_l\rangle \\ + C_{kl}^{xs}(\tau)\langle S_k\rangle\langle x_l\rangle + C_{kl}^x(\tau)\langle S_k\rangle\langle S_l\rangle. \quad (25)$$

For $k = l$ we obtain

$$Z_k(\tau) = A_k^s(\tau)\langle x_k\rangle\langle x_k\rangle + A_k^{sx}(\tau)\langle x_k\rangle\langle S_k\rangle \\ + A_k^{xs}(\tau)\langle S_k\rangle\langle x_k\rangle + A_k^x(\tau)\langle S_k\rangle\langle S_k\rangle. \quad (26)$$

Equations such as (22), (25), and (26) for the equal-time cross-correlations $C_{ij}^s(0)$ include correlation functions between neural activities and synaptic variables, such as C_{ij}^{sx}, C_{ij}^{xs}, C_{ij}^x, A_i^{sx}, A_i^{xs}, and A_i^x. We thus need the equations for these correlation functions between neural activities and synaptic variables to solve these equations.

Next, let us consider equal-time correlation functions $C_{ij}^{sx}(0)$, $C_{ij}^{xs}(0)$, $C_{ij}^x(0)$, $A_i^{sx}(0)$, $A_i^{xs}(0)$, and $A_i^x(0)$. Similar to the approach we took in calculating $C_{ij}^s(0)$, we obtain (see Appendix B for details)

$$C_{ij}^{sx}(0) = \sum_{\tau=1}^{\infty}\sum_{k\neq i,j}\tilde{J}_{ik}(\tau)\bigg\{\left(1-\frac{1}{\tau_d}\right)\big[C_{kj}^x(\tau-1)\langle S_k\rangle \\ + C_{kj}^{sx}(\tau-1)\langle x_k\rangle\big] - UZ_{kj}(\tau-1)\bigg\} \\ + \sum_{\tau=1}^{\infty}\tilde{J}_{ij}(\tau)\bigg\{\left(1-\frac{1}{\tau_d}\right)\big[A_j^x(\tau-1)\langle S_j\rangle \\ + A_j^{sx}(\tau-1)\langle x_j\rangle\big] - UZ_j(\tau-1)\bigg\}, \quad (27)$$

$$C_{ij}^x(0) = \left(1-\frac{1}{\tau_d}\right)^2 C_{ij}^x(0) + U^2 Z_{ij}(0) \\ - U\left(1-\frac{1}{\tau_d}\right)\big[C_{ij}^x(0)(\langle S_i\rangle + \langle S_j\rangle) \\ + C_{ij}^{sx}(0)\langle x_i\rangle + C_{ij}^{xs}(0)\langle x_j\rangle\big]. \quad (28)$$

Since $C_{ij}^{xs}(t,t) = C_{ji}^{sx}(t,t)$, we can also obtain $C_{ji}^{sx}(0)$ from Eq. (27). If we set $j = i$ in Eq. (27), we derive the equations for equal-time autocorrelations $A_i^{sx}(0)$,

$$A_i^{sx}(0) = \sum_{\tau=1}^{\infty}\sum_{k\neq i}\tilde{J}_{ik}(\tau)\bigg\{\left(1-\frac{1}{\tau_d}\right)\big[\langle x_k\rangle C_{ki}^{sx}(\tau-1) \\ + \langle S_k\rangle C_{ki}^x(\tau-1)\big] - UZ_{ki}(\tau-1)\bigg\}. \quad (29)$$

Since $A_i^{xs}(0) = A_i^{sx}(0)$, we simultaneously obtain $A_i^{xs}(0)$. Similarly, we set $i = j$ in Eq. (28) to obtain equal-time autocorrelation $A_i^x(0)$ as

$$A_i^x(0) = \left(1-\frac{1}{\tau_d}\right)^2 A_i^x(0) + U^2 Z_i(0) \\ - U\left(1-\frac{1}{\tau_d}\right)2\big[A_i^x(0)\langle S_i\rangle + A_i^{sx}(0)\langle x_i\rangle\big]. \quad (30)$$

Because $A_i^x(0)$ and $A_i^{sx}(0)$ are 1 and $1/N$ orders, respectively, we ignore $A_i^{sx}(0)$ and derive

$$A_i^x(0) = \frac{U^2 A_i^s(0)\langle x_i\rangle^2}{1-(1-1/\tau_d)^2 - U^2\langle S_i\rangle^2 + -2U(1-1/\tau_d)\langle S_i\rangle}. \quad (31)$$

These equations for equal-time cross-correlations $C_{ij}^s(0)$ and $C_{ij}^{sx}(0)$ and equal-time autocorrelations $A_i^{sx}(0)$ include time-delayed cross-correlations, such as $C_{ij}^s(\tau)$, $C_{ij}^{sx}(\tau)$, $C_{ij}^{xs}(\tau)$, and $C_{ij}^x(\tau)$, and time-delayed autocorrelations such as $A_i^s(\tau)$, $A_i^{sx}(\tau)$, $A_i^{xs}(\tau)$, and $A_i^x(\tau)$. We thus need the equations for these time-delayed correlation functions to solve these equations.

C. Time-delayed correlation functions

We derive the equations for the time-delayed correlation functions in this section Let us consider time-delayed cross-correlation functions between neural activities $C_{ij}^s(t, t + \tau)$. The time-delayed cross-correlation functions can be written as

$$C_{ij}^s(t, t+\tau) = \langle S_i(t) S_j(t+\tau)\rangle - \langle S_i(t)\rangle\langle S_j(t+\tau)\rangle \\ = \sum_{Y^{t+\tau-1}} P(Y^{t+\tau-1})S_i(t)\sum_{\mathbf{S}^{t+\tau}}[S_j(t+\tau) \\ \times W(\mathbf{S}^{t+\tau}|Y^{t+\tau-1}) - \langle S_i(t)\rangle\langle S_j(t+\tau)\rangle] \\ = \langle S_i(t)g[u_j(t+\tau)]\rangle - \langle S_i(t)\rangle\langle S_j(t+\tau)\rangle \\ = \langle\delta S_i(t)g[u_j(t+\tau)]\rangle. \quad (32)$$

By expanding $g[u_j(t+\tau)]$ around the noise average of u_j and taking in limit $t \to \infty$, we derive the time-delayed cross-correlation functions as

$$C_{ij}^s(\tau) = \sum_{\tau'=1}^{\infty}\sum_{k\neq j,i}\tilde{J}_{jk}(\tau')\big[C_{ik}^{sx}(\tau-\tau')\langle S_k\rangle + C_{ik}^s(\tau-\tau')\langle x_k\rangle\big] \\ + \sum_{\tau'=1}^{\infty}\tilde{J}_{ji}(\tau')\big[A_i^{sx}(\tau-\tau')\langle S_i\rangle + A_i^s(\tau-\tau')\langle x_i\rangle\big]. \quad (33)$$

If we set $j = i$ in Eq. (33), we obtain time-delayed autocorrelation functions between neural states $A_i^s(\tau)$ at equilibrium:

$$A_i^s(\tau) = \sum_{\tau'=1}^{\infty}\sum_{k\neq i}\tilde{J}_{ik}(\tau')\big[C_{ik}^{sx}(\tau-\tau')\langle S_k\rangle + C_{ik}^s(\tau-\tau')\langle x_k\rangle\big]. \quad (34)$$

Next we consider time-delayed cross-correlation functions between S_i and x_j, that is, $C_{ij}^{sx}(\tau)$. Substituting Eq. (3) into Eq. (17) and taking limit $t \to \infty$ gives

$$C_{ij}^{sx}(\tau) = \lim_{t\to\infty}\bigg\langle\delta S_i(t)\bigg\{\left(1-\frac{1}{\tau_d}\right)\delta x_j(t+\tau-1) \\ - U\delta[x_j(t+\tau-1)S_j(t+\tau-1)]\bigg\}\bigg\rangle \\ = \left(1-\frac{1}{\tau_d} - U\langle S_j\rangle\right)C_{ij}^{sx}(\tau-1) - U\langle x_j\rangle C_{ij}^s(\tau-1). \quad (35)$$

If we set $j = i$ in Eq. (35), we derive the time-delayed autocorrelation functions between S_i and x_i [$A_i^{sx}(\tau)$] as

$$A_i^{sx}(\tau) = \left(1 - \frac{1}{\tau_d} - U\langle S_i \rangle\right) A_i^{sx}(\tau - 1) - U\langle x_i \rangle A_i^s(\tau - 1). \tag{36}$$

Taking into account the order of $A_i^{sx}(\tau)$ and $A_i^s(\tau)$, we can simplify Eq. (36). $A_i^{sx}(0)$ and $A_i^{sx}(\tau)$ $(1 \leqslant \tau)$ are each on the order of $1/N$ and 1, while $A_i^s(0)$ and $A_i^s(\tau)$ $(1 \leqslant \tau)$ are on the order of 1 and $1/N$, respectively. Ignoring $A_i^{sx}(0)$ and $A_i^s(\tau)$ $(1 \leqslant \tau)$, we obtain
1, $\tau = 1$

$$A_i^{sx}(1) = -U\langle x_i \rangle A_i^s(0), \tag{37}$$

2, $\tau > 1$

$$A_i^{sx}(\tau) = \left(1 - \frac{1}{\tau_d} - U\langle S_i \rangle\right) A_i^{sx}(\tau - 1). \tag{38}$$

Similar to the approach we took in the previous section, time-delayed cross-correlation functions between x_i and S_j [$C_{ij}^{xs}(t, t + \tau)$] can be written as $C_{ij}^{xs}(t, t + \tau) = \langle \delta x_i(t) g[u_j(t + \tau)] \rangle$. By expanding $g[u_j(t + \tau)]$ around the noise average of u_j and taking in limit $t \to \infty$, we obtain

$$C_{ij}^{xs}(\tau) = \sum_{\tau'=1}^{\infty} \sum_{k \neq j, i} \tilde{J}_{jk}(\tau') \left[C_{ik}^x(\tau - \tau')\langle S_k \rangle + C_{ik}^{xs}(\tau - \tau')\langle x_k \rangle \right]$$
$$+ \sum_{\tau'=1}^{\infty} \tilde{J}_{ji}(\tau') \left[A_i^x(\tau - \tau')\langle S_i \rangle + A_i^{xs}(\tau - \tau')\langle x_i \rangle \right]. \tag{39}$$

If we set $j = i$ in Eq. (39), we obtain time-delayed autocorrelation functions between x_i and S_i [$A_i^{xs}(\tau)$] as

$$A_i^{xs}(\tau) = \sum_{\tau'=1}^{\infty} \sum_{k \neq i} \tilde{J}_{ik}(\tau') \left[C_{ik}^x(\tau - \tau')\langle S_k \rangle + C_{ik}^{xs}(\tau - \tau')\langle x_k \rangle \right]. \tag{40}$$

Finally, we derive time-delayed cross-correlation functions between x_i and x_j, that is, $C_{ij}^x(\tau)$. Substituting Eq. (3) into Eq. (17) and taking limit $t \to \infty$ gives

$$C_{ij}^x(\tau) = \lim_{t \to \infty} \left\langle \delta x_i(t) \left\{ \left(1 - \frac{1}{\tau_d}\right) \delta x_j(t + \tau - 1) \right. \right.$$
$$\left. \left. - U\delta[x_j(t + \tau - 1) S_j(t + \tau - 1)] \right\} \right\rangle$$
$$= \left(1 - \frac{1}{\tau_d} - U\langle S_j \rangle\right) C_{ij}^x(\tau - 1) - U\langle x_j \rangle C_{ij}^{xs}(\tau - 1). \tag{41}$$

If we set $j = i$ in Eq. (41), we obtain time-delayed autocorrelation functions between synaptic variables at equilibrium:

$$A_i^x(\tau) = \left(1 - \frac{1}{\tau_d} - U\langle S_i \rangle\right) A_i^x(\tau - 1), \tag{42}$$

where we ignore $A_i^{xs}(\tau - 1)$, because $A_i^x(\tau)$ and $A_i^{xs}(\tau - 1)$ are on the order of 1 and $1/N$, respectively. By solving Eqs. (20), (22), (27)–(29), (31), (33)–(35), and (37)–(42)

we eventually obtain the equilibrium value for correlations between the activities of cortical neurons and those between neural activities and synaptic variables.

D. Correlations of mean firing rate

We calculated the correlations of spikes $\langle \delta S_i \delta S_j \rangle$ in the previous section. Here we compute the correlation functions of the mean firing rate within time window T, $Q_{ij} = \langle \delta r_i \delta r_j \rangle$, where $\delta r_i \equiv r_i - \langle r_i \rangle$, and we call the value r_i, the mean firing rate. We calculate the rate correlations to evaluate the effect of synaptic depression on the correlations between neural activities within the long term T. Firing rate r_i and synaptic efficacy q_i within T is defined as

$$r_i = \frac{1}{T}\sum_{\tau=1}^{T} S_i(\tau), \quad q_i = \frac{1}{T}\sum_{\tau=1}^{T} x_i(\tau). \tag{43}$$

Mean firing rate f_i and mean synaptic efficacy X_i at equilibrium are the same as instantaneous firing rate $\langle S_i \rangle$ and instantaneous synaptic efficacy $\langle x_i \rangle$, respectively:

$$f_i \equiv \langle r_i \rangle = \frac{1}{T}\sum_{\tau=1}^{T} \langle S_i(\tau) \rangle = \langle S_i \rangle,$$
$$X_i \equiv \langle q_i \rangle = \frac{1}{T}\sum_{\tau=1}^{T} \langle x_i(\tau) \rangle = \langle x_i \rangle. \tag{44}$$

The correlation for the mean firing rate can be calculated as in Refs. [23,33]

$$Q_{ij} = \langle \delta r_i \delta r_j \rangle$$
$$= \langle (r_i - f_i)(r_j - f_j) \rangle$$
$$= \left\langle \left[\frac{1}{T}\sum_{\tau=1}^{T} S_i(\tau) - f_i \right] \left[\frac{1}{T}\sum_{\tau'=1}^{T} S_j(\tau') - f_j \right] \right\rangle$$
$$= \frac{1}{T^2}\sum_{\tau=1}^{T}\sum_{\tau'=1}^{T} \langle S_i(\tau) S_j(\tau') \rangle - f_i f_j$$
$$= \frac{1}{T^2}\sum_{\tau=1}^{T}\sum_{\tau'=1}^{T} [\langle \delta S_i(\tau) \delta S_j(\tau') \rangle + \langle S_i(\tau) \rangle \langle S_j(\tau') \rangle] - f_i f_j$$
$$= \frac{1}{T^2}\sum_{\tau=1}^{T}\sum_{\tau'=1}^{T} C_{ij}^s(\tau' - \tau). \tag{45}$$

Using mean firing rate correlations Q_{ij}, which can be computed though Eq. (45), we can evaluate the effect of synaptic depression on neural correlations over the long term.

E. Fisher information

Let us consider the problem of how accurately stimulus θ, which is a single variable, can be estimated from the mean firing rates of neuronal population $\mathbf{r} = \{r_1, r_2, \ldots, r_N\}$. Through the Cramer-Rao bound, the average squared decoding error for an unbiased estimation of stimulus $\hat{\theta}$ is greater than or equal to $1/I(\theta)$,

$$\langle (\theta - \hat{\theta})^2 \rangle \geqslant \frac{1}{I(\theta)}, \tag{46}$$

when $I(\theta)$ is Fisher information. Fisher information is given by

$$I(\theta) = \int d\mathbf{r} \, P[\mathbf{r}|\theta] \left(-\frac{\partial^2 \ln P[\mathbf{r}|\theta]}{\partial \theta^2} \right), \quad (47)$$

where $P[\mathbf{r}|\theta]$ is the conditional probability distribution, which is the probability that neural response $\mathbf{r}$ will be evoked by the presentation of a multivariate Gaussian probability distribution with covariance matrix $Q(\theta)$,

$$P[\mathbf{r}|\theta] = \frac{1}{\sqrt{(2\pi)^N \det \mathbf{Q}(\theta)}}$$
$$\times \exp\left\{ -\frac{1}{2}[\mathbf{r} - \mathbf{f}(\theta)]^T \mathbf{Q}^{-1}(\theta)[\mathbf{r} - \mathbf{f}(\theta)] \right\}, \quad (48)$$

where $\mathbf{f}$ is the mean value of $\mathbf{r}$. Note that the (i,j)th element of covariance matrix Q_{ij} represents mean firing rate correlation $\langle \delta r_i \delta r_j \rangle$. Under this assumption, Fisher information can be written as in Ref. [34]:

$$I(\theta) = I_{\text{mean}}(\theta) + I_{\text{cov}}(\theta), \quad (49)$$
$$I_{\text{mean}}(\theta) = \mathbf{f}'(\theta)^T \mathbf{Q}^{-1}(\theta) \mathbf{f}'(\theta), \quad (50)$$
$$I_{\text{cov}}(\theta) = \text{Tr}[\mathbf{Q}'(\theta)\mathbf{Q}^{-1}(\theta)\mathbf{Q}-1(\theta)]/2, \quad (51)$$

where Tr stands for the trace operation, $f'(\theta) = df(\theta)/d\theta$, and $\mathbf{Q}'(\theta) = d\mathbf{Q}/d\theta$. Because mean firing rates r and mean firing rate correlations Q_{ij} can be analytically calculated in the spike response model as discussed earlier in Sec. III D, Fisher information can also be analytically calculated from Eq. (49).

IV. RING ATTRACTOR NETWORK WITH MEXICAN-HAT-TYPE CONNECTIVITY

A. Model

Let us now consider a ring attractor neural network with Mexican-hat-type connectivity [26,27]. We do not do this to imply the presence of such ring structures in neuroanatomy, but merely to illustrate that neurons tuned to a periodic variable are functionally fully connected. This ring network model is thus not a one-dimensional lattice model but has often been used as an appropriately approximated network model of the primary visual cortex [26]. Following these previous studies, we used the conventional ring neural network model and investigated what effect synaptic depression had on neural correlations.

In this network, $N = 1000$ neurons are divided into a $K = 10$ subpopulation. The choice of the number of subpopulations does not qualitatively affect the results. The number of neurons in each population is $G = 100$. All neurons in each population have the same preferred orientation and neuron i in the kth population is labeled using angle θ_k. We assume that the preferred orientations of $K = 10$ subpopulations are evenly distributed from $-\pi/2$ to $\pi/2$, and divide 2π in $K = 10$, that is, $\theta_k = -\pi/2 + k\pi/K$. The strength of connections J_{kl} between a neuron in the kth population and a neuron in the lth population is calculated as

$$J_{kl} = J_0/N + J_1 \cos 2(\theta_k - \theta_l)/N, \quad (52)$$

where J_0 is a uniform interaction and J_1 is a lateral-inhibitory interaction. The model with $J_1 = 0$ is reduced to a network

with uniform connections. We set uniform interaction $J_0 = 0.5$ and lateral-inhibitory interaction $J_1 = 3$ to stabilize the steady states [25,31]. Neurons in simulations are evolved at maximum 10^3 time steps with initial state $S_i(0) = 0$ and $x_i(0) = 1 \; \forall i$, until they reach a stable equilibrium point. Instantaneous firing rates and correlation functions are estimated from simulations over 5×10^6 time steps in equilibrium.

B. Correlation functions

To investigate the effect of synaptic depression on neural correlations, we adjust the external inputs to neurons h_i and maintain the firing rate $\langle S_i(t) \rangle$ regardless of the strength of synaptic depression γ (see Appendix C). We set h_i as follows:

$$h_i = h_i^0 + \sum_{\tau}^{\infty} \sum_{j \neq i}^{N} J_{ij} \epsilon_{ij}(\tau) \frac{2\gamma \langle S_i^0 \rangle^2}{1 + \gamma \langle S_i^0 \rangle}, \quad (53)$$

where we define h_i^0 and $\langle S_i^0 \rangle$ as the respective input and instantaneous firing rate in the absence of synaptic depression, that is, $\gamma = 0$. We set $h_i^0 = f_0 \cos[2(\theta_i - \phi)]$, $f_0 = 0.05$, and the orientation of stimuli $\phi = 0$. Using self-consistent Eq. (15), we can derive $\langle S_i^0 \rangle$. We then adjust external inputs h_i and obtained constant firing rates regardless of synaptic depression, as can be seen in Figs. 1(a) and 1(b). In addition, each neuron follows a probabilistic dynamic depending on the firing probability $g[u_i(t)] = \frac{1}{2}\{1 + \tanh[\beta u_i(t)]\}$, where $1/\beta \; (=T)$ is the level of noise due to stochastic synaptic activity and we set $\beta = 1$ [23,27]. The response kernels of the discrete spike
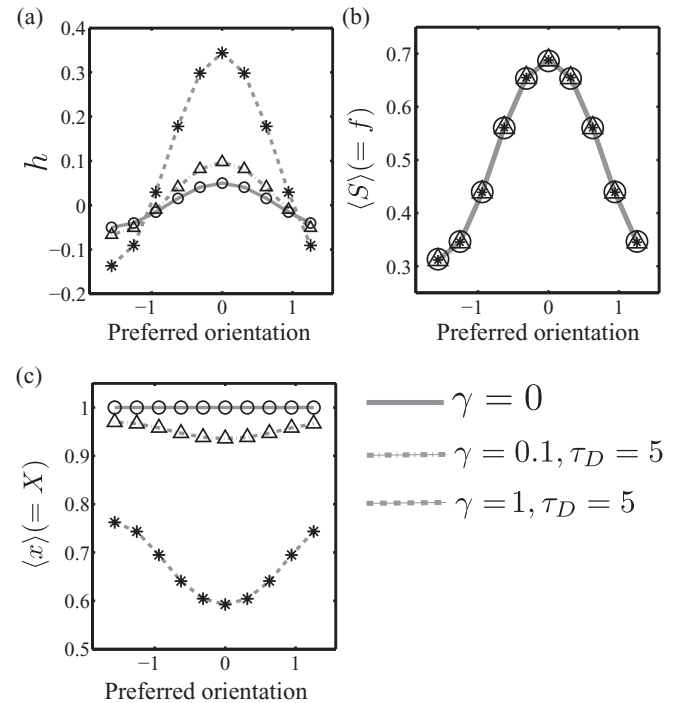

FIG. 1. (a) Inputs, (b) instantaneous firing rates $\langle S \rangle$, and (c) synaptic efficacy $\langle x \rangle$ obtained from simulations (open circles, triangles, and asterisks) compared with theory (solid lines) in absence and presence of synaptic depression, $\gamma = 0, 0.1$, and 1, respectively, with $\tau_D = 5$. Parameters of connections are $J_0 = 0.5$ and $J_1 = 3$.
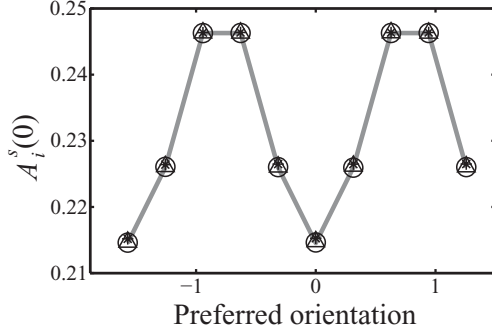
FIG. 2. Equal-time autocorrelation functions $A_i^s(0)$ obtained from simulations (open circles, triangles, and asterisks) compared with theory (solid, chain, and dotted lines) in absence and presence of synaptic depression, $\gamma = 0, 0.1,$ and 1, respectively, with $\tau_D = 5$. Because of firing rates in presence of synaptic depression as well as those in its absence [Fig. 1(b)], $A_i^s(0)$ agree completely with each other.

model are given by $\epsilon_{ij}(\tau) = [1 - \exp(-1/\tau_s)]\exp(-\tau/\tau_s)$, where $\tau_s = 2$.

We found that the firing correlations obtained under these conditions by using our theory coincided with the results from simulations, as seen in Figs. 2 and 3. Figure 2 shows equal-time autocorrelation functions $A_i^s(\tau)$ of a neuron with preferred orientations from $-\pi/2$ to $2\pi/5$. Equal-time autocorrelation functions $A_i^s(0)$ in absence of synaptic depression coincide with those in presence of synaptic depression (as indicated in Fig. 2) because the autocorrelation functions of neural activity depend on instantaneous firing rates Eq. (20) and the instantaneous firing rates for in the case of $\gamma = 0$ are the same as those for $\gamma = 0.1$ and 1 [Fig. 1(b)]. Let us then consider the results for time-delayed autocorrelations $A_i^s(\tau)$ where $\tau > 1$. Figure 3(a) plots the autocorrelation functions of a neuron with preferred orientation 0 rad. We found that the strength of synaptic depression γ increases and sequences of spikes are less correlated. The simulation results are in agreement with both those from the theoretical solution and a previous study [28].

Next, let us consider what effects synaptic depression has on neural cross-correlations between neurons. Figure 3(b)

plots the cross-correlation functions between a neuron with preferred orientation 0 rad and a neuron with preferred orientation $\pi/10$ rad where $J_{ik} > 0$. For $J_{ik} > 0$, $C_{ij}^s(\tau) > 0$ because the synaptic strength between the neurons is positive regardless of synaptic depression. We found that synaptic depression reduces $C_{ij}^s(\tau)$. Next, we will discuss how depressing synapses affect $C_{ij}^s(\tau)$ where $J_{ik} < 0$. Figure 3(c) plots the cross-correlation functions between a neuron with preferred orientation 0 rad and a neuron with preferred orientation $\pi/2$ rad where synaptic connection $J_{ik} < 0$. Since the synaptic strength between the neurons is negative, $C_{ij}^s(\tau) < 0$ regardless of synaptic depression. We found that synaptic depression increases cross-correlation $C_{ij}^s(\tau)$.

Using correlation theory to solve self-consistent equations in a network with synaptic depression enables us to understand how synaptic depression quantitatively affects neural correlation. As shown in Fig. 3, neural activities gradually decorrelate depending on the strength of synaptic depression γ and the reductions in neural correlations are quite large for weak depression $\gamma = 0.1$. We thus found that synaptic depression nonlinearly decorrelates neural activities in the entire network with synaptic depression.

C. Rate correlation

We explained that depressing synapses reduces spiking correlations $A^s(\tau)$ and $C^s(\tau)$ at almost all τ in the previous section. We calculated rate correlation r_i using Eq. (45) to evaluate what effect synaptic depression had on the neural correlation between neural activities within a long time frame. When we calculated the firing rate correlation between a neuron with preferred orientation 0 rad and a neuron with preferred orientation $\pi/10$, we found that synaptic depression reduces rate correlations r_i by 98% for $\gamma = 1$.

Next, let us consider the effect of depressing synapses on all the pair-wise correlations of neural activities. The correlation theory in a network with synaptic depression enables us to investigate entire rate correlation $\mathbf{Q}$, as shown in Fig. 4.

Here, to visualize the $\mathbf{Q}$ of neurons, let us introduce a $K \times K$ matrix $\mathcal{Q}$, where $K = 10$ is the number of subpopulations in the neurons. Because the correlations between two neurons
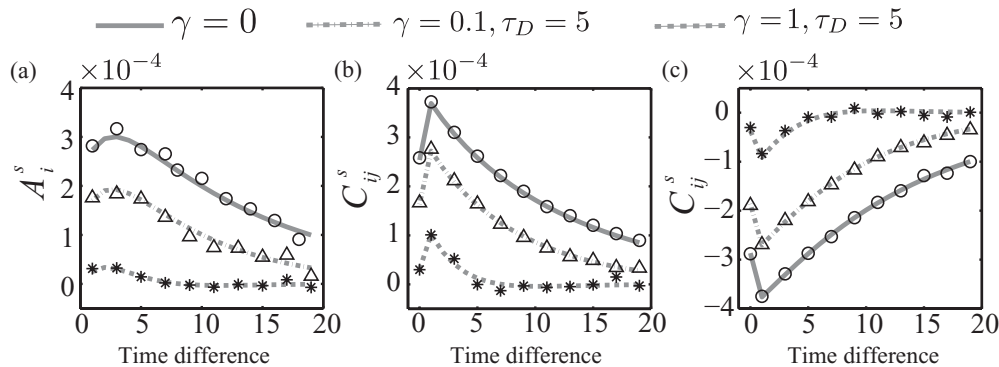

FIG. 3. Autocorrelation and cross-correlation functions from simulations (open circles, triangles, and asterisks) compared with theory (solid, chain, and dotted lines) in absence and presence of synaptic depression, $\gamma = 0, 0.1,$ and 1, respectively, with $\tau_D = 5$. (a) Autocorrelation functions of neuron with preferred orientation 0 rad [$A_i^s(\tau)$] where $\tau > 1$. (b) Cross-correlation functions between neuron i with preferred orientation 0 rad and neuron j with preferred orientation $\pi/10$ rad [$C_{ij}^s(\tau)$], where $J_{ij} > 0$. (c) Cross-correlation functions between neuron i with preferred orientation 0 rad and neuron j with preferred orientation $\pi/2$ rad [$C_{ij}^s(\tau)$], where $J_{ij} < 0$.
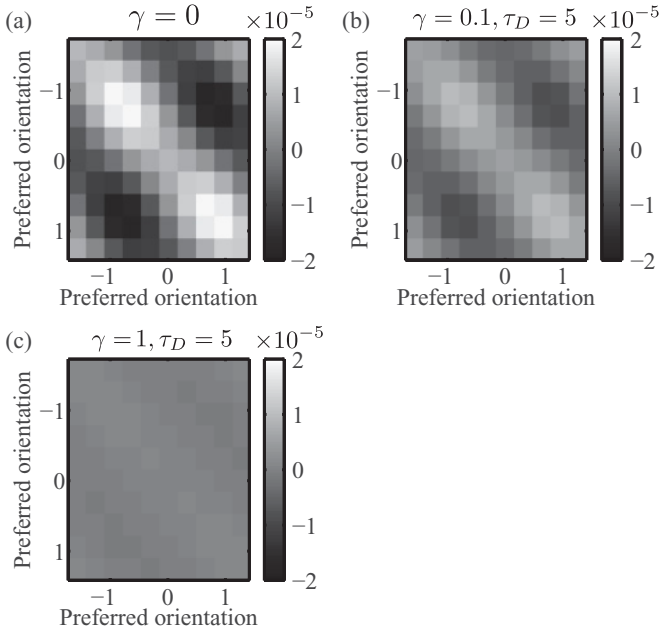
FIG. 4. (a) Grayscale plots of covariance matrix $\mathcal{Q}$ in absence of synaptic depression ($\gamma = 0$), (b) in presence of weak synaptic depression ($\gamma = 0.1$ and $\tau_D = 5$), and (c) strong synaptic depression ($\gamma = 1$ and $\tau_D = 5$).
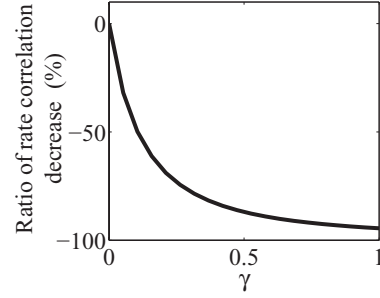

FIG. 5. Effects of synaptic depression on average of absolute value of rate correlations.

$\mathbf{Q}^{-1}$. Because synaptic depression changes both $\mathbf{f}'$ and $\mathbf{Q}^{-1}$, we have to take both changes into account to consider how synaptic depression affects the amount of information.

We adjusted inputs h_i in Secs. IV B and IV C, and maintained mean firing rates $\mathbf{f}$ (as shown in Fig. 6) to consider what effect synaptic depression had on neural correlations. This section considers the effects of synaptic depression on both firing rates and neural correlations; we set external inputs $h_i = h_i^0$, where $h_i^0 = e_0 \cos[2(\theta_i - \phi)]$, $e_0 = 0.2$, and orientation stimuli $\phi = 0$. The response kernels of the discrete spike model are given by $\epsilon_{ij}(\tau) = [1 - \exp(-1/\tau_s)]\exp(-\tau/\tau_s)$, where $\tau_s = 2$. Synaptic depression generally reduces mean
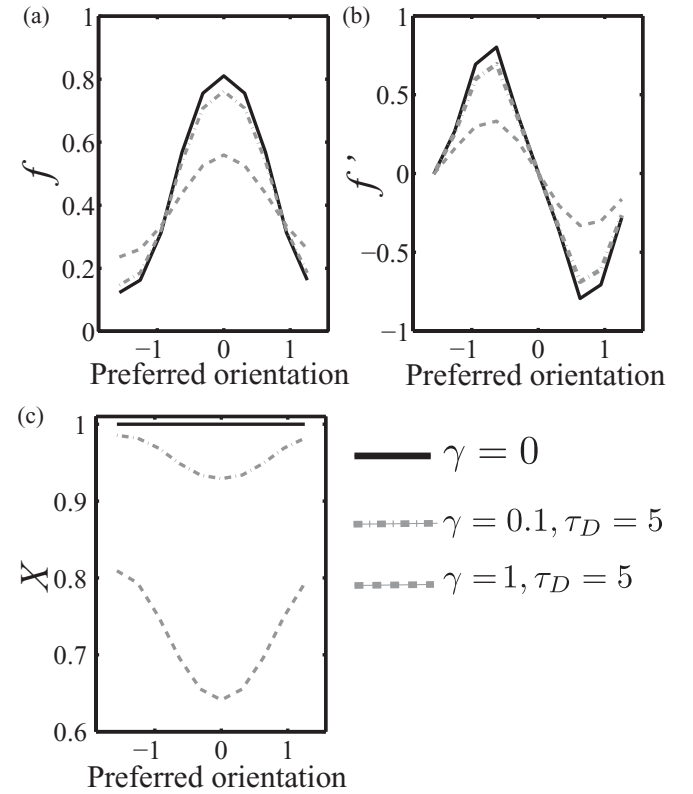
are only determined by the difference in their preferred orientations, the correlations between a neuron in the kth population of excitatory neurons and a neuron in the lth are the same. Thus, matrix $\mathbf{Q}$ can be written as $K \times K$ block matrix $\mathcal{Q}$. The elements of $\mathcal{Q}$, and $\mathcal{Q}_{kl}$, stand for the mean firing rate correlations between a neuron in the kth population of neurons and one in the lth:

$$\mathcal{Q}_{kl} = Q_{ij}, \tag{54}$$

where $\forall\, i$ is in the kth population and $\forall\, j$ is in the lth; $\mathcal{Q}$ does not contain any diagonal elements of $\mathbf{Q}$. Although matrix $\mathbf{Q}$ is an $N \times N$ matrix, it is difficult to numerically calculate the entire matrix because of the substantial amount of time that would be required to do this. Note that our theoretical framework enables us to analytically calculate all pair-wise neural correlations. Figure 4 shows that the absolute values of all the pair-wise neural correlations greatly decrease depending on the strength of synaptic depression γ. Thus, neural activities decorrelate due to depressing synapses in an entire network. Finally, we investigate how neural activities decorrelate by changing the strength of synaptic depression. Figure 5 indicates that the greater the strength of synaptic depression γ, the fewer the rate correlations.

D. Fisher information

To understand what effect synaptic depression has on Fisher information I, which depends on firing rates and rate correlations, let us consider the first term of Fisher information $I_{\text{mean}} = \mathbf{f}'(\theta)^T \mathbf{Q}^{-1} \mathbf{f}'(\theta)$, because I_{mean} is foremost in our model (the second term of Fisher information I_{cov} is only about 0.7% of the Fisher information I). I_{mean} depends on the derivatives of mean firing rates $\mathbf{f}'$ and the inverse of covariance matrix

FIG. 6. (a) Mean firing rates f, (b) derivatives of mean firing rates f', and (c) mean synaptic efficacies X of V1 neurons with $J_0 = 0.5$ and $J_1 = 3$. Solid lines plot f, f', and X in absence of synaptic depression ($\gamma = 0$ and $\tau_D = 1$). Chain and dashed lines plot f, f', and X in presence of weak synaptic depression ($\gamma = 0.1$ and $\tau_D = 5$) and strong synaptic depression ($\gamma = 1$ and $\tau_D = 5$), respectively.
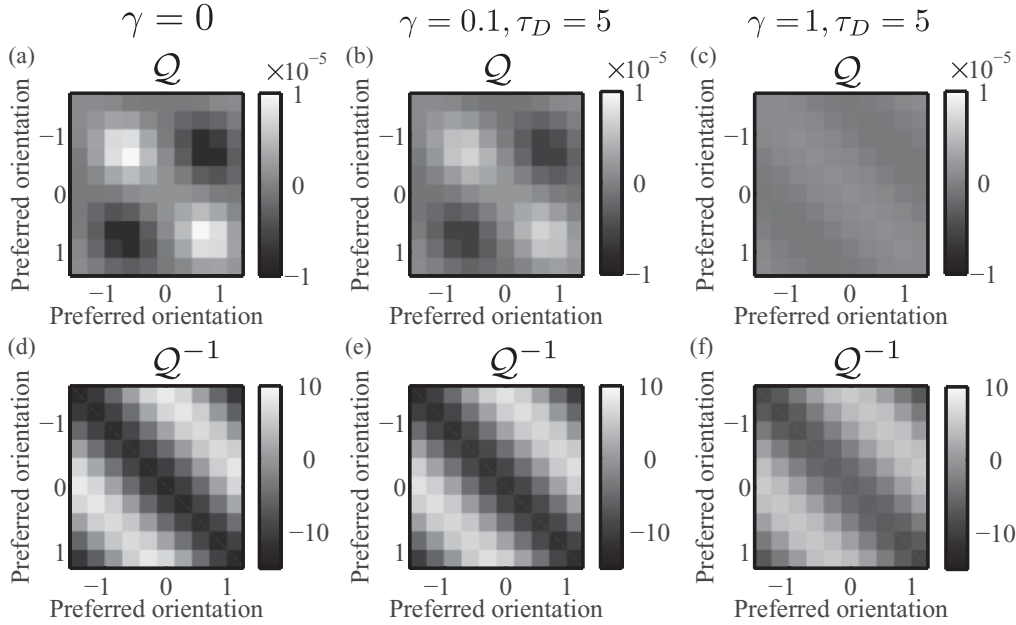
FIG. 7. Covariance matrix $\mathcal{Q}$ and those of inverse of covariance matrix $\mathcal{Q}^{-1}$. Note that off-diagonal elements of covariance matrix $\mathbf{Q}$ are written as $\mathcal{Q}$. (a)–(f) Plots of covariance matrix $\mathcal{Q}$ [(a), (b), and (c)] and inverse of covariance matrix $\mathcal{Q}^{-1}$ [(d), (e), and (f)] of V1 neurons in the absence ($\gamma = 0$) and presence of weak ($\gamma = 0.1$ and $\tau_D = 5$) and strong ($\gamma = 1$ and $\tau_D = 5$) synaptic depression, respectively. Synaptic strengths are $J_0 = 0.5$ and $J_1 = 3$. Diagonal elements are set to 0 to enable visualization.

firing rates $\mathbf{f}$ and their slopes ($\mathbf{f}' = d\mathbf{f}/d\theta$), as shown in Figs. 6(a) and 6(b) [2,25]. These changes to the firing rates reduce $I_{\text{mean}} = \mathbf{f}'(\theta)^T \mathbf{Q}^{-1} \mathbf{f}'(\theta)$.

Now we shall consider how $\mathbf{Q}^{-1}$ affects Fisher information. Figures 7(a)–7(f) show the off-diagonal elements of covariance matrix $\mathbf{Q}$ and those of the inverse of covariance matrix $\mathbf{Q}^{-1}$. When locally positive correlations are induced by recurrent excitations [Figs. 7(a)–7(c)], the off-diagonal elements of $\mathbf{Q}^{-1}$ near the diagonal elements are negative [Figs. 7(d)–7(f)]. As demonstrated by Eq. (50), we can understand that these locally negative off-diagonal elements decrease Fisher information if the tuning curves $\mathbf{f}$ are fixed. Locally positive correlations thus decrease Fisher information [12]. Next, let us investigate how synaptic depression affects $\mathbf{Q}^{-1}$. As discussed in Sec. IV C, synaptic depression reduces rate correlations $\mathbf{Q}$ [Figs. 7(a)–7(c)]. Neural decorrelation also leads to an increase in locally

negative off-diagonal elements, as indicated in Figs. 7(d)–7(f), which increases the amount of information.

As a result, the effects of the derivatives of the tuning curves $\mathbf{f}'$ on Fisher information are the opposite of the effects of neural correlations. Whether Fisher information increases or not as a combinational effect is determined by which effects are stronger. We calculated the Fisher information to evaluate the effects of synaptic depression on information processing and found that, when we set the parameters for connections, $J_0 = 0.5$ and $J_1 = 3$, synaptic depression increased the amount of information depending on the strength of synaptic depression shown in Fig. 8. However, synaptic depression does not always increase Fisher information, because it depends on the synaptic strengths J_0 and J_1. We also found that synaptic depression reduced Fisher information for the weak lateral-inhibitory interaction $J_1 = 1$ shown in Fig. 9. Thus, synaptic connections established the effect of synaptic depression.
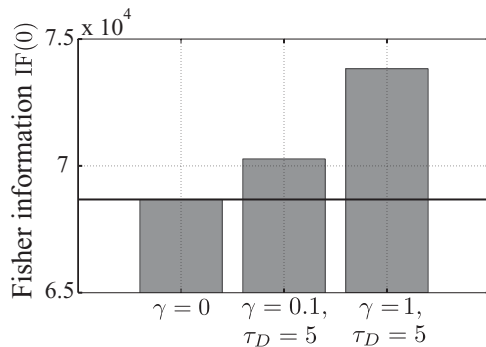

FIG. 8. Effects of synaptic depression on Fisher information. Fisher information increases depending on strength depression γ, when parameters of connections are $J_0 = 0.5$ and $J_1 = 3$.
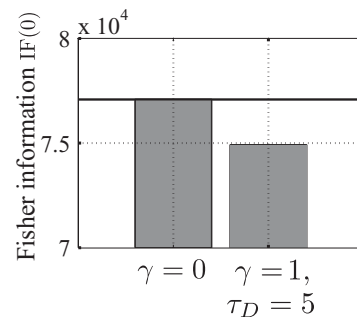

FIG. 9. Effects of synaptic depression on Fisher information. When we set uniform interaction $J_0 = 0.5$ and weak lateral-inhibitory interaction $J_1 = 1$ synaptic depression ($\gamma = 1$ and $\tau_D = 5$) decreases Fisher information by 2.8%.

V. DISCUSSION

We constructed a theory of correlation in spiking neuron models with synaptic depression by expanding a previous theoretical framework [20–23]. This theory enables us to analytically calculate what effect synaptic depression, which rapidly changes neural interactions, had on neural correlations. Our study should open up the way for theoretical studies on the effects of interaction changes on the linear response function in large stochastic networks.

We investigated how synaptic depression affects neural correlations in a ring attractor network with Mexican-hat-type connectivity by using our theoretical framework. We found that synaptic depression reduces neural cross correlations in the ring network model as well as neural autocorrelations by using our theoretical framework [28]. The decorrelations of neural activities can improve the efficiency of a population of neurons encoding information [11,14–16].

To evaluate how synaptic depression affects information processing, we analytically calculated Fisher information, which quantifies the maximum amount of information on stimuli that can be extracted from noisy neural activities. We found that although synaptic depression generally reduces signal strength, viz., the mean firing rates, it can improve the efficiency of population coding. Some researchers have reported that short-term synaptic depression is a possible mechanism for the effects of belief adaptation to a stimulus with a fixed orientation in the primary visual cortex, because this brief adaptation leads to the depression of feed forward synapses and intracortical synapses [9,35]. In fact, recent neurophysiological experiments have shown that, after belief adaptation, both firing rates and neural correlations decrease and Fisher information increases in the macaque primary visual cortex [15]. These post-adaptation changes coincide with the effects of synaptic depression. Further investigations are needed to calculate Fisher information in the network of the primary visual cortex with synaptic depression [35] to enable the mechanism for decorrelation after brief adaptation to be studied.

Recent findings by Montani *et al.* and Ohiorhenuan and Victor have pointed out the relevance of higher order correlations that are larger than two in the cerebral cortex [36,37]. Macke *et al.* have theoretically proved that common inputs explain high-order correlations in a simple model of neural population activity [38], in which there were no recurrent connections and neural correlations were only determined by common inputs. In contrast, we did not consider common noisy inputs in our model for simplicity, which produced large high-order correlations, and focused on neural correlations which were produced only by recurrent synaptic connections. We therefore could analytically calculate the neural correlations and theoretically prove that the pair-wise correlations are scaled as $\sim O(1/N)$ and that high-order correlations are less than the order of $1/N$ in a network with synaptic depression, where N is the number of neurons. On the other hand, we cannot directly argue how synaptic depression affects the large higher-order correlations produced by common inputs in the framework of the mean-field theory. Further study

will be to include common noisy inputs in the network and investigate by simulations what effect synaptic depression has on higher correlations, which are produced by common inputs.

We have only investigated the role of synaptic depression in spike train decorrelation in this study, but other short-term processes such as spike rate adaptation [39], synaptic facilitation [3,40], and postsynaptic receptor dynamics could enable more general filtering of spike trains [41]. Mongillo *et al.* reported that working memory is sustained by both synaptic depression and synaptic facilitation in the recurrent connections of neocortical networks [42]. However, neural correlations, which affect the efficiency of a population of neurons to encode information, have not been taken into consideration in the network. Expanding our theoretical framework to spiking neural network models with both synaptic depression and facilitation and investigating how these synaptic plasticities affect Fisher information is an interesting issue that we intend to pursue.

APPENDIX A: THE ORDER OF INPUT CORRELATIONS

We prove that $\langle (\delta u_i)^2 \rangle$ is the order of $1/N$ in this Appendix. Using Eqs. (22), (25), and (26), we can write $\langle (\delta u_i)^2 \rangle$ as

$$\langle (\delta u_i)^2 \rangle = \Bigg\langle \sum_{\tau,\tau'}^{\infty} \sum_{j \neq i} \sum_{k \neq i} 2J_{ij}\epsilon_{ij}(\tau) 2J_{ik}\epsilon_{ik}(\tau')$$

$$\times \delta[x_j(t-\tau)S_j(t-\tau)]\delta[x_k(t-\tau')S_k(t-\tau')] \Bigg\rangle,$$

$$= \sum_{\tau,\tau'}^{\infty} \sum_{j \neq i} \sum_{k \neq i,j} 2J_{ij}\epsilon_{ij}(\tau) 2J_{ik}\epsilon_{ik}(\tau') Z_{jk}(t-\tau, t-\tau')$$

$$+ \sum_{\tau,\tau'}^{\infty} \sum_{j \neq i} 4J_{ij}^2 \epsilon_{ij}(\tau)\epsilon_{ij}(\tau') Z_j(t-\tau, t-\tau'). \quad \text{(A1)}$$

First we consider the order of the first term in Eq. (A1). When each neuron is connected to a number of neurons of order N and connections J_{ij} are all of order $1/N$, $\sum_{\tau,\tau'}^{\infty} \sum_{j \neq i} \sum_{k \neq i,j} 2J_{ij}\epsilon_{ij}(\tau) 2J_{ik}\epsilon_{ik}(\tau')$ are of order 1 and the order of the first term in Eq. (A1) is determined by $Z_{jk}(t-\tau, t-\tau')$. Using Eq. (26), we found $Z_{jk}(t-\tau, t-\tau')$ $(j \neq k)$ is the same order of $1/N$ as C_{jk}^s. Thus, the order of the first term in Eq. (A1) is $1/N$. Next, we discuss the order or the second term in Eq. (A1). Similarly, because $J_{ij}^2 \epsilon_{ij}(\tau)\epsilon_{ij}(\tau')$ are of order $1/N$ and the order of $Z_j(t-\tau, t-\tau')$ is no more than the order of $O(1)$, the second term in Eq. (A1) is also on the order of $1/N$. Hence, the order of $\langle (\delta u_i)^2 \rangle$ is $1/N$.

APPENDIX B: EQUAL-TIME CORRELATION FUNCTIONS

Here we describe the details on calculating equal-time correlation functions. A important point in the calculations is that we ignore high-order correlations, which are no more than the order of $1/N$, to derive a set of closed equations for correlation functions.

First, we derive the equal-time cross-correlation functions between $S_i(t)$ and $S_j(t)$ $(j \neq i)$ at equilibrium $C_{ij}^s(0)$ [Eq. (22)]. By expanding $g[u_i(t)]$ around the noise average of $\langle u_i \rangle$ [Eq. (21)], we obtain

$$C_{ij}^s(0) = g'(\langle u_i \rangle) g'(\langle u_j \rangle) \langle \delta u_i \delta u_j \rangle, \tag{B1}$$

where $\langle \delta u_i \delta u_j \rangle$ is

$$\langle \delta u_i \delta u_j \rangle = \sum_{\tau,\tau'} \sum_{k \neq i} \sum_{l \neq j,k} 2 J_{ik} \epsilon_{ik}(\tau) 2 J_{jl} \epsilon_{jl}(\tau') Z_{kl}(\tau - \tau')$$
$$+ \sum_{\tau,\tau'} \sum_{k \neq i} 2 J_{ik} \epsilon_{ik}(\tau) 2 J_{jk} \epsilon_{jk}(\tau') Z_k(\tau - \tau'), \tag{B2}$$

because

$$\delta u_i(t) = \sum_{\tau=1}^{\infty} \sum_{j \neq i} J_{ij} \epsilon_{ij}(\tau) 2 \delta[(x_j(t-\tau) S_j(t-\tau)]. \tag{B3}$$

Substituting Eq. (B2) into Eq. (B1) gives Eq. (22).

We then evaluate $Z_{kl}(\tau)$ and $Z_k(\tau)$ as discussed above. $Z_{kl}(t, t + \tau)$ can be written as

$$Z_{kl}(t, t+\tau) = \langle \delta[x_k(t) S_k(t)] \delta[x_l(t+\tau) S_l(t+\tau)] \rangle,$$
$$= \langle x_k(t) S_k(t) x_l(t+\tau) S_l(t+\tau) \rangle$$
$$- \langle x_k(t) S_k(t) \rangle \langle x_l(t+\tau) S_l(t+\tau) \rangle,$$
$$= \langle [\delta x_k(t) + \langle x_k(t) \rangle][\delta S_k(t) + \langle S_k(t) \rangle]$$
$$\times [\delta x_l(t+\tau) + \langle x_l(t+\tau) \rangle]$$
$$\times [\delta S_l(t+\tau) + \langle S_l(t+\tau) \rangle] \rangle$$
$$- \langle [\delta x_k(t) + \langle x_k(t) \rangle][\delta S_k(t) + \langle S_k(t) \rangle] \rangle$$
$$= C_{kl}^s(t, t+\tau) \langle x_k(t) \rangle \langle x_l(t+\tau) \rangle$$
$$+ C_{kl}^{sx}(t, t+\tau) \langle x_k(t) \rangle \langle S_l(t+\tau) \rangle$$
$$+ C_{kl}^{xs}(t, t+\tau) \langle S_k(t) \rangle \langle x_l(t+\tau) \rangle$$
$$+ C_{kl}^x(t, t+\tau) \langle S_k(t) \rangle \langle S_l(t+\tau) \rangle. \tag{B4}$$

We ignore three-point cross correlations and four-point cross correlations. Taking limit $t \to \infty$ yields Eq. (25). For $k = l$ in Eq. (25) we obtain Eq. (26).

Next, let us consider equal-time cross-correlation functions between S_i and x_j [$C_{ij}^{sx}(0)$]. Similar to the approach we took in the previous section, we expanded $g[u_i(t)]$ around $\langle u_i \rangle$ and

substituted it into Eq. (3) to obtain

$$C_{ij}^{sx}(t,t) = \left\langle g'[\langle u_i(t) \rangle] \delta u_i(t) \left\{ \left(1 - \frac{1}{\tau_d} \right) \delta x_j(t-1) \right. \right.$$
$$\left. \left. - U \delta[x_j(t-1) S_j(t-1)] \right\} \right\rangle$$
$$= \sum_{\tau=1}^{\infty} \sum_{k \neq i,j} \tilde{J}_{ik}(\tau) \left\{ \left(1 - \frac{1}{\tau_d} \right) \times \langle \delta[x_k(t-\tau) \right.$$
$$\left. \times S_k(t-\tau)] \delta x_j(t-1) \rangle - U Z_{kj}(t-\tau, t-1) \right\}, \tag{B5}$$

where we denote $\tilde{J}_{ik}(\tau) = 2 g'(\langle u_i \rangle) J_{ik} \epsilon_{ik}(\tau)$ and use Eq. (24). Taking limit $t \to \infty$ gives

$$C_{ij}^{sx}(0) = \lim_{t \to \infty} \sum_{\tau=1}^{\infty} \sum_{k \neq i,j} \tilde{J}_{ik}(\tau) \left\{ \left(1 - \frac{1}{\tau_d} \right) \times \langle \delta[(x_k(t-\tau) \right.$$
$$\left. \times S_k(t-\tau)] \delta x_j(t-1) \rangle - U Z_{kj}(\tau-1) \right\}. \tag{B6}$$

To derive a set of closed equations for correlation functions, which is described by Eqs. (18) and (19), we evaluate $\lim_{t \to \infty} \langle \delta[(x_k(t-\tau) S_k(t-\tau)] \delta x_j(t-1) \rangle$ as

$$\lim_{t \to \infty} \langle \delta[x_k(t-\tau) S_k(t-\tau)] \delta x_i(t-1) \rangle$$
$$= \lim_{t \to \infty} \langle x_k(t-\tau) S_k(t-\tau) \delta x_i(t-1) \rangle$$
$$= \lim_{t \to \infty} \langle \{\delta[x_k(t-\tau)] + \langle x_k(t-\tau) \rangle\}\{\delta[(S_k(t-\tau)]$$
$$+ \langle S_k(t-\tau) \rangle\} \delta x_i(t-1) \rangle$$
$$= \langle x_k \rangle C_{ki}^{sx}(\tau-1) + \langle S_k \rangle C_{ki}^x(\tau-1). \tag{B7}$$

Substituting Eq. (B7) into Eq. (B6) gives Eq. (27). Since $C_{ij}^{xs}(t,t) = C_{ji}^{sx}(t,t)$, we can also obtain $C_{ij}^{xs}(0)$ from Eq. (27).

Finally, we derive equal-time cross-correlation functions between x_i and x_j [$C_{ij}^x(0)$]. Substituting Eq. (3) into Eq. (17) and taking limit $t \to \infty$ gives

$$C_{ij}^x(0) = \lim_{t \to \infty} \left\{ \left(1 - \frac{1}{\tau_d} \right) \delta x_i(t-1) - U \delta[x_i(t-1) S_i(t-1)] \right\}$$
$$\times \left\{ \left(1 - \frac{1}{\tau_d} \right) \delta x_j(t-1) - U \delta[x_j(t-1) S_j(t-1)] \right\}$$
$$= \lim_{t \to \infty} \left(\left(1 - \frac{1}{\tau_d} \right)^2 C_{ij}^x(t-1, t-1) \right.$$
$$+ U^2 Z_{ij}(t-1, t-1) - U \left(1 - \frac{1}{\tau_d} \right)$$
$$\times \{ \langle \delta[x_i(t-1) S_i(t-1)] \delta x_j(t-1) \rangle$$
$$\left. + \langle \delta[x_j(t-1) S_j(t-1)] \delta x_i(t-1) \rangle \} \right). \tag{B8}$$

Substituting Eq. (B7) into Eq. (B8) we obtain Eq. (28).

APPENDIX C: ADJUSTMENT OF EXTERNAL INPUTS

We first explain why we have to maintain the firing rate $\langle S_i \rangle$ in order to study how synaptic depression affects neural correlations in this Appendix. While the change in instantaneous firing rates affects neural correlations Eq. (20), input h_i only has an indirect effect on neural correlations via the instantaneous firing rates. We thus adjust the strength of input and maintain the firing rate to study what effects synaptic depression has on neural correlations.

We then derive the external inputs to neurons h_i. To begin with, we simply emulate noisy orientation selective inputs to the neurons [Fig. 1(a)]. We respectively define h_i^0 and $\langle S_i^0 \rangle$ as the input and instantaneous firing rate in the absence of synaptic depression, that is, $\gamma = 0$. To keep $\langle S_i \rangle$ in the presence of synaptic depression γ the same as $\langle S_i^0 \rangle$ by changing h_i, we derive the following equation from the self-consistent equation (15):

$$
g \left[\sum_{\tau=1}^{\infty} \sum_{j \neq i} J_{ij} \epsilon_{ij}(\tau) \left(2 \frac{\langle S_j^0 \rangle}{1 + \gamma \langle S_j^0 \rangle} - 1 \right) + h_i + u_r \right]
$$

$$
= g \left[\sum_{\tau=1}^{\infty} \sum_{j \neq i} J_{ij} \epsilon_{ij}(\tau) \left(2 \langle S_j^0 \rangle - 1 \right) + h_i^0 + u_r \right]. \quad \text{(C1)}
$$

Since the escape function g monotonically increases, Eq. (C1) can be written as Eq. (53). Using Eq. (53), we adjust external inputs h_i and the instantaneous firing rates for $\gamma = 0$ to the same as those for $\gamma = 0.1$ and 1 shown in Fig. 1. Note from Eq. (44) that instantaneous firing rate $\langle S_i \rangle$ and instantaneous synaptic efficacy $\langle x_i \rangle$ are the same as mean firing rate f_i and mean synaptic efficacy X_i, respectively, at equilibrium.

---

[1] A. M. Thomson and J. Deuchars, Trends Neurosci. **17**, 119 (1994).

[2] L. Abbott, J. Varela, K. Sen, and S. Nelson, Science **275**, 221 (1997).

[3] M. Tsodyks, K. Pawelzik, and H. Markram, Neural Comput. **10**, 821 (1998).

[4] L. E. Dobrunz and C. F. Stevens, Neuron **22**, 157 (1999).

[5] J. A. Varela, K. Sen, J. Gibson, J. Fost, L. F. Abbott, and S. B. Nelson, J. Neurosci. **17**, 7926 (1997).

[6] R. S. Zucker and W. G. Regehr, Annu. Rev. Physiol. **64**, 355 (2002).

[7] L. Abbott and W. Regehr, Nature (London) **431**, 796 (2004).

[8] M. Tsodyks and C. Gilbert, Nature (London) **431**, 775 (2004).

[9] A. Kohn, J. Neurophysiol. **97**, 3155 (2007).

[10] E. Zohary, M. N. Shadlen, and W. T. Newsome, Nature (London) **370**, 149 (1994).

[11] L. F. Abbott and P. Dayan, Neural Comput. **11**, 91 (1999).

[12] H. Sompolinsky, H. Yoon, K. Kang, and M. Shamir, Phys. Rev. E **64**, 051904 (2001).

[13] P. Series, P. E. Latham, and A. Pouget, Nat. Neurosci. **7**, 1129 (2004).

[14] B. B. Averbeck, P. E. Latham, and A. Pouget, Nat. Rev. Neurosci. **7**, 358 (2006).

[15] D. A. Gutnisky and V. Dragoi, Nature (London) **452**, 220 (2008).

[16] M. R. Cohen and J. H. R. Maunsell, Nat. Neurosci. **12**, 1594 (2009).

[17] J. M. Cortes, D. Marinazzo, P. Series, M. W. Oram, T. J. Sejnowski, and M. C. W. van Rossum, J. Comput. Neurosci. (in press).

[18] R. J. Glauber, J. Math. Phys. **4**, 294 (1963).

[19] M. Suzuki and R. Kubo, J. Phys. Soc. Jpn. **24**, 51 (1968).

[20] I. Ginzburg and H. Sompolinsky, Phys. Rev. E **50**, 3171 (1994).

[21] C. Meyer and C. van Vreeswijk, Neural Comput. **14**, 369 (2001).

[22] T. Toyoizumi, K. R. Rad, and L. Paninski, Neural Comput. **21**, 1203 (2009).

[23] M. Oizumi, K. Miura, and M. Okada, Phys. Rev. E **81**, 051905 (2010).

[24] Y. Igarashi, M. Oizumi, Y. Otsubo, K. Nagata, and M. Okada, J. Phys. Conf. Ser. **197**, 012018 (2009).

[25] Y. Igarashi, M. Oizumi, and M. Okada, J. Phys. Soc. Jpn. **79**, 084001 (2010).

[26] R. Ben-Yishai, R. Bar-Or, and H. Sompolinsky, Proc. Natl. Acad. Sci. USA **92**, 3844 (1995).

[27] K. Hamaguchi, J. P. L. Hatchett, and M. Okada, Phys. Rev. E **73**, 051104 (2006).

[28] M. S. Goldman, P. Maldonado, and L. F. Abbott, J. Neurosci. **22**, 584 (2002).

[29] W. Gerstner and J. L. van Hemmen, Network: Computation in Neural Systems **3**, 139 (1992).

[30] W. Gerstner and W. Kistler, *Spiking Neuron Models* (Cambridge University Press, New York, 2002).

[31] L. C. York and M. C. W. van Rossum, J. Comput. Neurosci. **27**, 607 (2009).

[32] Z. P. Kilpatrick and P. C. Bressloff, Physica D **239**, 547 (2010).

[33] J. H. Macke, P. Berens, A. S. Ecker, and A. S. Tolias, Neural Comput. **21**, 397 (2009).

[34] S. M. Kay, *Fundamentals of Statistical Signal Processing: Estimation Theory* (Cambridge University Press, Prentice-Hall, Englewood Cliffs, NJ, 1993).

[35] M. I. Chelaru and V. Dragoi, Cereb. Cortex **18**, 771 (2008).

[36] F. Montani, R. A. A. Ince, R. Senatore, E. Arabzadeh, M. E. Diamond, and S. Panzeri, Phil. Trans. R. Ser. A **367**, 3297 (2009).

[37] I. E. Ohiorhenuan and J. D. Victor, J. Comput. Neurosci. **30**, 125 (2011).

[38] J. H. Macke, M. Opper, and M. Bethge, Phys. Rev. Lett. **106**, 208102 (2011).

[39] Y. H. Liu and X. J. Wang, J. Comput. Neurosci. **10**, 25 (2001).

[40] J. E. Lisman, Trends Neurosci. **20**, 383 (1997).

[41] W. Maass and A. M. Zador, Neural Comput. **11**, 903 (1999).

[42] G. Mongillo, O. Barak, and M. Tsodyks, Science **319**, 1543 (2008).